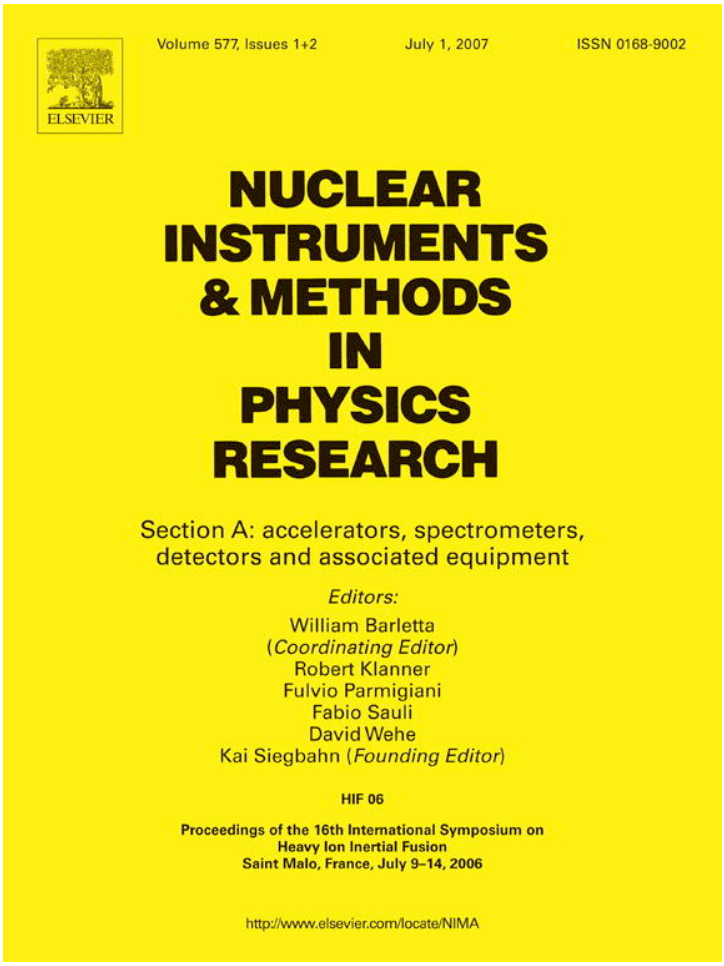

Available online at www.sciencedirect.com
ScienceDirect
Nuclear Instruments and Methods in Physics Research A 577 (2007) 70–78
NUCLEAR INSTRUMENTS & METHODS IN PHYSICS RESEARCH Section A
www.elsevier.com/locate/nima

Multispecies Weibel instability for intense charged particle beam propagation through neutralizing background plasma

Ronald C. Davidson[a,*], Igor Kaganovich[a], Edward A. Startsev[a], Hong Qin[a], Mikhail Dorf[a], Adam Sefkow[a], Dale R. Welch[b], David V. Rose[b], Steven M. Lund[c]

[a]*Plasma Physics Laboratory, Princeton University, Princeton, New Jersey, USA*
[b]*Voss Scientific, Albuquerque, New Mexico, USA*
[c]*Lawrence Livermore National Laboratory, University of California, California, USA*

Available online 24 February 2007

Abstract

Properties of the multi-species electromagnetic Weibel instability are investigated for an intense ion beam propagating through background plasma. Assuming that the background plasma electrons provide complete charge and current neutralization, detailed linear stability properties are calculated within the framework of a macroscopic cold-fluid model for a wide range of system parameters.

PACS: 41.75.Ak; 52.59.Fn

Keywords: Ion beams; Beam–plasma interactions; Instabilities

1. Introduction

High energy ion accelerators, transport systems and storage rings [1,2] are used in fundamental research in high energy physics and nuclear physics, and in applications such as ion-beam driven high energy density physics and fusion, spallation neutron sources, and nuclear waste transmutation. Charged particle beams at high intensities are often subject to various collective processes that can deteriorate the beam quality. Therefore, it is increasingly important to develop a detailed theoretical understanding of the linear and nonlinear dynamics of intense charged particle beams and beam–plasma systems, with the goal of identifying operating regimes that minimize the deleterious effects of collective processes on beam transport and focusing. Considerable progress has been made in recent theoretical investigations [3–6], often with the aid of advanced numerical simulations. These investigations include a wide variety of collective interaction processes, ranging from the electrostatic Harris instability [7–13] and the electromagnetic Weibel instability [14–19] driven by large temperature anisotropy with $T_{\perp b} \gg T_{\parallel b}$ in a one-component nonneutral ion beam, to wall-impedance-driven collective instabilities [20–22], to the dipole-mode two-stream instability (electron cloud instability) for an intense ion beam propagating through a partially neutralizing electron background [4,23–30], to the resistive hose instability [31–36], the sausage and hollowing instabilities [37–39], and the multispecies two-stream and Weibel instabilities [3,40–45], for an intense ion beam propagating through a background plasma [46–52].

In the plasma plug and target chamber regions for ion-beam-driven high energy density physics and fusion applications [46–52], the intense ion beam experiences collective interactions with the background plasma. In this paper, we investigate theoretically detailed properties of the multi-species electromagnetic Weibel instability for an intense ion beam propagating through background plasma [3,42,44]. Assuming that the background plasma electrons provide complete charge and current neutralization, detailed linear stability properties are calculated within the framework of a macroscopic cold-fluid model for a wide range of system parameters. Finally, the theoretical

*Corresponding author. Tel.: +1 609 243 3552.
E-mail address: rdavidson@pppl.gov (R.C. Davidson).

0168-9002/$ - see front matter © 2007 Elsevier B.V. All rights reserved.
doi:10.1016/j.nima.2007.02.036

formalism developed in this paper can also be applied to the case of an intense relativistic electron beam propagating through a dense background plasma, which is of considerable interest for investigations of the multispecies Weibel instability in applications pertaining to fast ignition [53–55] using high-intensity short-pulse lasers [56].

The organization of this paper is the following. The assumptions and theoretical model are described in Section 2. The eigenvalue equation for the multispecies Weibel instability is then analyzed in Section 3.

2. Macroscopic fluid model and eigenvalue equation

In the present analysis, we make use of a macroscopic fluid model [1,57] to describe the interaction of an intense ion beam ($j = b$) with background plasma electrons and ions ($j = e, i$). The charge and rest mass of a particle of species j ($j = b, e, i$) are denoted by e_j and m_j, respectively. In equilibrium, the steady-state ($\partial/\partial t = 0$) average flow velocities are taken to be in the z-direction, $\mathbf{V}_j^0(\mathbf{x}) = V_{zj}^0(r)\hat{\mathbf{e}}_z = \beta_j(r)c\hat{\mathbf{e}}_z$, and cylindrical symmetry is assumed ($\partial/\partial\theta = 0$). Axial motions are generally allowed to be relativistic, and the directed axial kinetic energy is denoted by $(\gamma_j - 1)m_jc^2$, where $\gamma_j(r) = [1 - \beta_j^2(r)]^{-1/2}$ is the relativistic mass factor of a fluid element. Furthermore, the analysis is carried out in the paraxial approximation, treating the velocity spread of the beam particles as small in comparison with $\beta_b c$. Denoting the equilibrium density profile by $n_j^0(r)$ ($j = b, e, i$), the corresponding equilibrium self-electric field, $\mathbf{E}^0(\mathbf{x}) = E_r^0(r)\hat{\mathbf{e}}_r$, and azimuthal self-magnetic field, $\mathbf{B}^0(\mathbf{x}) = B_\theta^0(r)\hat{\mathbf{e}}_\theta$, are determined self-consistently from

$$\frac{1}{r}\frac{\partial}{\partial r}r\frac{\partial}{\partial r}E_r^0(r) = \sum_{j=b,e,i} 4\pi e_j n_j^0(r) \tag{1}$$

$$\frac{1}{r}\frac{\partial}{\partial r}r\frac{\partial}{\partial r}B_\theta^0(r) = \sum_{j=b,e,i} 4\pi e_j \beta_j(r) n_j^0(r) \tag{2}$$

where $r = (x^2 + y^2)^{1/2}$ is the radial distance from the axis of symmetry. Finally, denoting the transverse pressure by $P_{\perp j}^0(r) = n_j^0(r)T_{\perp j}^0(r)$, equilibrium radial force balance on a fluid element of species j corresponding to a self-pinched equilibrium is given by

$$\frac{\partial}{\partial r}P_{\perp j}^0(r) = n_j^0(r)e_j[E_r^0(r) - \beta_j(r)B_\theta^0(r)]. \tag{3}$$

Examples of specific equilibrium profiles consistent with Eqs. (1)–(3) are given in Chapter 10 of Ref. [1].

In the macroscopic stability analysis of the multi-species Weibel instability presented here [3,42], we specialize to the case of axisymmetric, electromagnetic perturbations with $\partial/\partial\theta = 0$ and $\partial/\partial z = 0$, and perturbed quantities are expressed as $\delta\psi(r, t) = \delta\psi(r)\exp(-i\omega t)$ where $\mathrm{Im}\,\omega > 0$ corresponds to instability (temporal growth). For the perturbations, the perturbed field components are $\boldsymbol{\delta E}(\mathbf{x}, t) = \delta E_r(r, t)\hat{\mathbf{e}}_r + \delta E_z(r, t)\hat{\mathbf{e}}_z$ and $\boldsymbol{\delta B}(\mathbf{x}, t) = \delta B_\theta(r, t)\hat{\mathbf{e}}_\theta$, where

$$-\frac{i\omega}{c}\delta B_\theta(r) = \frac{\partial}{\partial r}\delta E_z(r) \tag{4}$$

follows from the θ-component of the $\nabla \times \boldsymbol{\delta E}$ Maxwell equation. Furthermore, some straightforward algebra shows that the r- and z-components of the $\nabla \times \boldsymbol{\delta B}$ Maxwell equation can be expressed as

$$\left(\frac{1}{r}\frac{\partial}{\partial r}r\frac{\partial}{\partial r} + \frac{\omega^2}{c^2}\right)\delta E_z(r) = -\frac{4\pi i\omega}{c^2}\left(\sum_{j=b,e,i} e_j n_j^0(r)\delta V_{zj}(r) + \sum_{j=b,e,i} e_j\beta_j(r)c\delta n_j(r)\right) \tag{5}$$

$$\frac{\omega^2}{c^2}\delta E_r(r) = -\frac{4\pi i\omega}{c^2}\sum_{j=b,e,i} e_j n_j^0(r)\delta V_{rj}(r) \tag{6}$$

where δV_{zj}, δV_{rj} and δn_j are determined self-consistently in terms of δE_z from the linearized continuity and force-balance equations. Note from Eqs. (4)–(6) that the field perturbations have mixed polarization with both a longitudinal component ($\delta E_r \neq 0$) and transverse electromagnetic field components ($\delta B_\theta \neq 0$ and $\delta E_z \neq 0$). This is because for drifting charge components with $\beta_j \neq 0$ the electrostatic and ordinary-mode electromagnetic perturbations are coupled.

With regard to the linearized continuity and force balance equations, in the present macroscopic analysis we neglect the effects of pressure perturbations. Denoting the density and average momentum of a fluid element of species j by $n_j = n_j^0 + \delta n_j$ and $\mathbf{P}_j = \gamma_j m_j \beta_j c\hat{\mathbf{e}}_z + \boldsymbol{\delta P}_j$, respectively, the linearized continuity and force balance equations can be expressed as

$$-i\omega\delta n_j + \frac{1}{r}\frac{\partial}{\partial r}(rn_j^0\delta V_{rj}) = 0 \tag{7}$$

$$-i\omega\delta P_{rj} = -e_j\left(-\delta E_r + \frac{1}{c}\delta V_{zj}B_\theta^0 + \beta_j\delta B_\theta\right) \tag{8}$$

$$-i\omega\delta P_{zj} = e_j\left(\delta E_z + \frac{1}{c}\delta V_{rj}B_\theta^0\right) \tag{9}$$

where $\delta P_{\theta j} = 0$ and $\beta_j(r)c = V_{zj}^0(r)$. Here, we can express $\delta\mathbf{P}_j = \gamma_j m_j \delta\mathbf{V}_j + \delta\gamma_j m_j\beta_j c\hat{\mathbf{e}}_z$, where $\delta\gamma_j = (\gamma_j^3/c^2)\mathbf{V}_j^0 \cdot \delta\mathbf{V}_j = (\gamma_j^3/c)\beta_j\delta V_{zj}$ and $\gamma_j = (1 - \beta_j^2)^{-1/2}$, which gives the expected results $\delta P_{rj} = \gamma_j m_j \delta V_{rj}$ and $\delta P_{zj} = \gamma_j^3 m_j \delta V_{zj}$.

It has been shown previously that a sufficiently strong self-magnetic field $B_\theta^0 \neq 0$ tends to reduce the growth rate of the Weibel instability in intense beam–plasma systems [58]. For our purposes here, in the remainder of this paper we specialize to the case of a charge-neutralized and current-neutralized beam–plasma system with

$$\sum_{j=b,e,i} n_j^0(r)e_j = 0, \quad \sum_{j=b,e,i} n_j^0(r)\beta_j e_j = 0 \tag{10}$$

where β_j is taken to be independent of r for simplicity. It then follows from Eqs. (1), (2) and (10) that $E_r^0 = 0 = B_\theta^0$, which is consistent with Eq. (3) in the cold-fluid limit.

Setting $B_\theta^0(r) = 0$ in Eqs. (5)–(9) gives

$$\mathrm{i}\omega\delta V_{rj} = -\frac{e_j}{\gamma_j m_j}\left(\delta E_r - \frac{\mathrm{i}c\beta_j}{\omega}\frac{\partial}{\partial r}\delta E_z\right) \tag{11}$$

$$\mathrm{i}\omega\delta V_{zj} = -\frac{e_j}{\gamma_j^3 m_j}\delta E_z \tag{12}$$

for the perturbed flow velocities. Combining Eqs. (6) and (11) then gives

$$\left[\omega^2 - \sum_{j=b,e,i}\omega_{pj}^2(r)\right]\delta E_r = -\frac{\mathrm{i}c}{\omega}\left(\sum_{j=b,e,i}\beta_j\omega_{pj}^2(r)\right)\frac{\partial}{\partial r}\delta E_z \tag{13}$$

where $\omega_{pj}^2(r) = 4\pi n_j^0(r)e_j^2/\gamma_j m_j$ is the relativistic plasma frequency-squared. Note that Eq. (13) relates the longitudinal electric field δE_r directly to $(\partial/\partial r)\delta E_z$. It is clear from Eq. (13) that $\delta E_r \neq 0$ whenever $\sum_{j=b,e,i}\beta_j\omega_{pj}^2 \neq 0$. From Eqs. (4), (11) and (13), we then obtain for the perturbed radial flow velocity

$$-\mathrm{i}\omega\gamma_j m_j\delta V_{rj} = -e_j\left[\beta_j + \frac{\sum_{j=b,e,i}\beta_j\omega_{pj}^2(r)}{\omega^2 - \sum_{j=b,e,i}\omega_{pj}^2(r)}\right]\frac{\mathrm{i}c}{\omega}\frac{\partial}{\partial r}\delta E_z. \tag{14}$$

Making use of Eqs. (7), (12) and (14) to express δV_{zj} and δn_j directly in terms of δE_z and $(\partial/\partial r)\delta E_z$, some straightforward algebra shows that the Maxwell equation (5) can be expressed as [42]

$$\frac{1}{r}\frac{\partial}{\partial r}\left[r\left(1 + \sum_{j=b,e,i}\frac{\beta_j^2\omega_{pj}^2(r)}{\omega^2} + \frac{(\sum_{j=b,e,i}\beta_j\omega_{pj}^2(r))^2}{\omega^2 - \sum_{j=b,e,i}\omega_{pj}^2(r)}\right)\frac{\partial}{\partial r}\delta E_z\right] + \left(\frac{\omega^2}{c^2} - \sum_{j=b,e,i}\frac{\omega_{pj}^2(r)}{\gamma_j^2 c^2}\right)\delta E_z = 0 \tag{15}$$

where $\gamma_j = (1-\beta_j^2)^{-1/2}$ is the relativistic mass factor, and $\omega_{pj}^2(r) = 4\pi n_j^0(r)e_j^2/\gamma_j m_j$.

Eq. (15) is the desired eigenvalue equation for axisymmetric, electromagnetic perturbations with polarization $\boldsymbol{\delta E} = \delta E_r\hat{\mathbf{e}}_r + \delta E_z\hat{\mathbf{e}}_z$ and $\boldsymbol{\delta B} = \delta B_\theta\hat{\mathbf{e}}_\theta$, with the terms proportional to $\sum_{j=b,e,i}\beta_j^2\omega_{pj}^2(r)$ and $\sum_{j=b,e,i}\beta_j\omega_{pj}^2(r)$ providing the free energy to drive the Weibel instability. Eq. (15) can be integrated numerically to determine the eigenvalue ω^2 and eigenfunction $\delta E_z(r)$ for a wide range of beam–plasma density profiles $n_j^0(r)$. As discussed in Section 3, analytical solutions are also tractable for the case of flat-top (step-function) density profiles. As a general remark, when $\sum_{j=b,e,i}\beta_j^2\omega_{pj}^2(r) \neq 0$ and $\sum_{j=b,e,i}\beta_j\omega_{pj}^2(r) \neq 0$, Eq. (15) supports both stable fast-wave solutions ($\mathrm{Im}\,\omega = 0$, $|\omega/ck_\perp| > 1$) and unstable slow-wave solutions ($\mathrm{Im}\,\omega > 0$, $|\omega/ck_\perp| < 1$). Here, $|k_\perp| \sim |\partial/\partial r|$ is the characteristic radial wavenumber of the perturbation. Moreover, Eq. (15) also supports stable plasma oscillation solutions with predominantly longitudinal polarization associated with the factor proportional to $[\omega^2 - \sum_{j=b,e,i}\omega_{pj}^2(r)]^{-1}$. Finally, for a perfectly conducting cylindrical wall located at $r = r_w$, the eigenvalue equation (15) is to be solved subject to the boundary condition

$$\delta E_z(r = r_w) = 0. \tag{16}$$

3. Multispecies Weibel instability for step-function density profiles

As an example that is analytically tractable, we consider the case illustrated in Fig. 1 where the density profiles are uniform both inside and outside the beam with

$$n_j^0(r) = \hat{n}_j^{\mathrm{i}} = \text{const.}, \quad j = b, e, i \tag{17}$$

for $0 \leqslant r < r_b$, and

$$n_j^0(r) = \hat{n}_j^{\mathrm{o}} = \text{const.}, \quad j = e, i \tag{18}$$

for $r_b < r \leqslant r_w$. Here, the superscript "i" ("o") denotes inside (outside) the beam, and $\hat{n}_b^{\mathrm{o}} = 0$ is assumed. Consistent with Eq. (10), $\sum_{j=b,e,i}\hat{n}_j^{\mathrm{i}}e_j = 0 = \sum_{j=b,e,i}\hat{n}_j^{\mathrm{i}}\beta_j e_j$ and $\sum_{j=e,i}\hat{n}_j^{\mathrm{o}}e_j = 0 = \sum_{j=e,i}\hat{n}_j^{\mathrm{o}}\beta_j e_j$ are assumed. We also take $\beta_j = 0$ $(j = e, i)$ in the region outside the beam $(r_b < r \leqslant r_w)$. The subsequent analysis of the eigenvalue equation (15) is able to treat the three cases: (a) beam–plasma-filled waveguide $(r_b = r_w)$; (b) vacuum region outside the beam $(r_b < r_w$ and $\hat{n}_j^{\mathrm{o}} = 0, j = e, i)$; and (c) plasma outside the beam $(r_b < r_w$ and $\hat{n}_j^{\mathrm{o}} \neq 0, j = e, i)$.

Referring to Fig. 1 and Eq. (15), it is convenient to introduce the constant coefficients

$$T_i^2(\omega) = \left[\frac{\omega^2}{c^2} - \sum_{j=b,e,i}\frac{\hat{\omega}_{pj}^{i2}}{\gamma_j^2 c^2}\right]\times\left[1 + \sum_{j=b,e,i}\frac{\beta_j^2\hat{\omega}_{pj}^{i^2}}{\omega^2} + \frac{(\sum_{j=b,e,i}\beta_j\hat{\omega}_{pj}^{i^2})^2}{\omega^2[\omega^2 - \sum_{j=b,e,i}\hat{\omega}_{pj}^{i^2}]}\right]^{-1} \tag{19}$$

for $0 \leqslant r < r_b$, and

$$T_o^2(\omega) = -\left[\frac{\omega^2}{c^2} - \sum_{j=e,i}\frac{\hat{\omega}_{pj}^{\mathrm{o}2}}{c^2}\right] \tag{20}$$

for $r_b < r \leqslant r_w$, where $\hat{\omega}_{pj}^{i2} = 4\pi\hat{n}_j^i e_j^2/\gamma_j m_j$, $j = b, e, i$, and $\hat{\omega}_{pj}^{\mathrm{o}2} = 4\pi\hat{n}_j^{\mathrm{o}}e_j^2/m_j$, $j = e, i$. We denote the eigenfunction inside the beam $(0 \leqslant r < r_b)$ by $\delta E_z^I(r)$, and the eigenfunction outside the beam $(r_b < r \leqslant r_w)$ by $\delta E_z^{II}(r)$. Eqs. (15), (19)

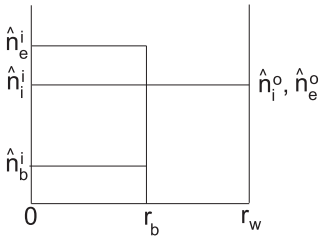

Fig. 1. Schematics of the density profiles of the beam ions ($\hat{n}_b^{\mathrm{i}}$) and the plasma ions and electrons inside ($\hat{n}_i^{\mathrm{i}}$ and $\hat{n}_e^{\mathrm{i}}$) and outside ($\hat{n}_i^{\mathrm{o}}$ and $\hat{n}_e^{\mathrm{o}}$) the beam.

and (20) then give

$$\frac{1}{r}\frac{\partial}{\partial r}\, r\, \frac{\partial}{\partial r}\, \delta E_z^I + T_i^2 \delta E_z^I = 0, \quad 0 \leqslant r < r_b \tag{21}$$

and

$$\frac{1}{r}\frac{\partial}{\partial r}\, r\, \frac{\partial}{\partial r}\, \delta E_z^{II} - T_o^2 \delta E_z^{II} = 0, \quad r_b < r \leqslant r_w \tag{22}$$

in the two regions. Eqs. (21) and (22) are Bessel's equations of order zero. The solutions to Eqs. (21) and (22) that are regular at $r = 0$, continuous at $r = r_b$, and vanish at the conducting wall are given by [42]

$$\delta E_z^I(r) = A J_0(T_i r), \quad 0 \leqslant r < r_b \tag{23}$$

$$\delta E_z^{II}(r) = A J_0(T_i r_b)\, \frac{K_0(T_o r_w) I_0(T_o r) - K_0(T_o r) I_0(T_o r_w)}{K_0(T_o r_w) I_0(T_o r_b) - K_0(T_o r_b) I_0(T_o r_w)}, \quad r_b < r \leqslant r_w \tag{24}$$

where A is a constant, $J_0(x)$ is the Bessel function of the first kind of order zero, and $I_0(x)$ and $K_0(x)$ are modified Bessel functions of order zero.

The remaining boundary condition is obtained by integrating the eigenvalue equation (15) across the beam surface at $r = r_b$. Making use of Eqs. (17) and (18), and assuming $\beta_e = 0 = \beta_i$ in the region outside the beam ($r_b < r \leqslant r_w$), we operate on Eq. (14) with $\int_{r_b(1-\varepsilon)}^{r_b(1+\varepsilon)} \mathrm{d}r r \cdots$ for $\varepsilon \to 0_+$. This readily gives the boundary condition

$$\left(1 + \sum_{j=b,e,i} \frac{\beta_j^2 \hat{\omega}_{pj}^{i2}}{\omega^2} + \frac{(\sum_{j=b,e,i} \beta_j \hat{\omega}_{pj}^{i^2})^2}{\omega^2[\omega^2 - \sum_{j=b,e,i} \hat{\omega}_{pj}^{i^2}]}\right) \left[\frac{\partial}{\partial r}\, \delta E_z^I\right]_{r=r_b} = \left[\frac{\partial}{\partial r} \delta E_z^{II}\right]_{r=r_b} \tag{25}$$

which relates the change in $\delta B_\theta = (\mathrm{i}c/\omega)(\partial \delta E_z/\partial r)$ at $r = r_b$ to the perturbed surface current. Substituting Eqs. (23) and (24) into Eq. (25) then gives

$$\left(1 + \sum_{j=b,e,i} \frac{\beta_j^2 \hat{\omega}_{pj}^{i2}}{\omega^2} + \frac{(\sum_{j=b,e,i} \beta_j \hat{\omega}_{pj}^{i^2})^2}{\omega^2[\omega^2 - \sum_{j=b,e,i} \hat{\omega}_{pj}^{i^2}]}\right) T_i r_b\, \frac{J_0'(T_i r_b)}{J_0(T_i r_b)} = T_o r_b\, \frac{K_0(T_o r_w) I_0'(T_o r_b) - K_0'(T_o r_b) I_0(T_o r_w)}{K_0(T_o r_w) I_0(T_o r_b) - K_0(T_o r_b) I_0(T_o r_w)} \tag{26}$$

where $T_i(\omega)$ and $T_o(\omega)$ are defined in Eqs. (19) and (20), and $I_0'(x) = (\mathrm{d}/\mathrm{d}x) I_0(x)$, $J_0'(x) = (\mathrm{d}/\mathrm{d}x) J_0(x)$, etc.

Eq. (26) constitutes a closed transcendental dispersion relation that determines the complex oscillation frequency ω for electromagnetic perturbations about the step-function profiles in Eqs. (17) and (18). As noted earlier, the dispersion relation has both fast-wave and slow-wave (Weibel-type) solutions, as well as a predominantly longitudinal (modified plasma oscillation) solution, and can be applied to the case of a beam–plasma-filled waveguide, or to the case where the region outside the beam ($r_b < r \leqslant r_w$) corresponds to vacuum ($\hat{n}_j^o = 0, j = e, i$) or background plasma ($\hat{n}_j^o \neq 0,\ j = e, i$).

3.1. Beam–plasma-filled waveguide ($r_b = r_w$)

For the case where the beam–plasma system extends to the conducting wall ($r_b = r_w$), the solution $\delta E_z^I(r) = A J_0(T_i r)$ in Eq. (23) is applicable over the entire interval $0 \leqslant r \leqslant r_w$. Applying the boundary condition $\delta E_z^I(r = r_w) = 0$ then gives the dispersion relation

$$J_0(T_i r_w) = 0 \tag{27}$$

which also follows from Eq. (26) in the limit $r_b \to r_w$. We denote by p_{0n} the nth zero of $J_0(p_{0n}) = 0$, and introduce the effective perpendicular wavenumber (quantized) defined by $k_\perp^2 = p_{0n}^2/r_w^2, n = 1, 2, \ldots$. The solutions to Eq. (27) are then determined from

$$T_i^2(\omega) = k_\perp^2, \quad n = 1, 2, \ldots \tag{28}$$

or equivalently,

$$1 + \sum_{j=b,e,i} \frac{\beta_j^2 \hat{\omega}_{pj}^{i2}}{\omega^2} + \frac{(\sum_{j=b,e,i} \beta_j \hat{\omega}_{pj}^{i^2})^2}{\omega^2[\omega^2 - \sum_{j=b,e,i} \hat{\omega}_{pj}^{i^2}]} = \frac{\omega^2}{c^2 k_\perp^2} - \sum_{j=b,e,i} \frac{\hat{\omega}_{pj}^{i2}}{\gamma_j^2 c^2 k_\perp^2} \tag{29}$$

where use has been made of Eq. (19). In the absence of axial flow ($\beta_j = 0$, $j = b, e, i$), note that the solution to Eq. (29) leads to the familiar fast-wave solution $\omega^2 = c^2 k_\perp^2 + \sum_{j=b,e,i} \omega_{pj}^{i2}$ with $\gamma_j = 1$. For $\sum_j \beta_j^2 \hat{\omega}_{pj}^{i2} \neq 0$ and $\sum_j \beta_j \hat{\omega}_{pj}^{i^2} \neq 0$, however, Eq. (29) supports two other solutions corresponding to the Weibel instability and plasma oscillation solution.

Eq. (29) is a cubic equation for ω^2. It is convenient to introduce the dimensionless quantities Ω^2, $K_\perp^2$, $\langle \beta^2 \rangle$ and $\langle \beta \rangle$ defined by

$$\Omega^2 = \frac{\omega^2}{\sum_{j=b,e,i} \hat{\omega}_{pj}^{i^2}}, \quad K_\perp^2 = \frac{c^2 k_\perp^2}{\sum_{j=b,e,i} \hat{\omega}_{pj}^{i^2}}$$
$$\langle \beta^2 \rangle = \frac{\sum_{j=b,e,i} \beta_j^2 \hat{\omega}_{pj}^{i^2}}{\sum_{j=b,e,i} \hat{\omega}_{pj}^{i^2}}, \quad \langle \beta \rangle = \frac{\sum_{j=b,e,i} \beta_j \hat{\omega}_{pj}^{i^2}}{\sum_{j=b,e,i} \hat{\omega}_{pj}^{i^2}}. \tag{30}$$

Rearranging terms, the dispersion relation (29) for a beam–plasma-filled waveguide can be expressed as

$$K_\perp^2[\Omega^4 - \Omega^2(1 - \langle \beta^2 \rangle) + (\langle \beta \rangle^2 - \langle \beta^2 \rangle)] = [\Omega^2 - (1 - \langle \beta^2 \rangle)]\Omega^2(\Omega^2 - 1) \tag{31}$$

where use has been made of $\sum_{j=b,e,i} \hat{\omega}_{pj}^{i^2}/\gamma_j^2 = (1 - \langle \beta^2 \rangle) \sum_{j=b,e,i} \hat{\omega}_{pj}^{i^2}$. In the absence of axial streaming ($\beta_j = 0$ and $\langle \beta \rangle = 0 = \langle \beta^2 \rangle$), the dispersion relation (31) gives directly the fast wave solution, $\Omega^2 = 1 + K_\perp^2$, or equivalently, $\omega^2 = c^2 k_\perp^2 + \sum_{j=b,e,i} \hat{\omega}_{pj}^{i^2}$, as expected. On the other hand, for $\langle \beta^2 \rangle \neq 0$ and $\langle \beta \rangle \neq 0$, and sufficiently short-wavelength perturbations that $K_\perp^2 = c^2 k_\perp^2 / \sum_{j=b,e,i} \hat{\omega}_{pj}^{i^2} \gg 1$, the dispersion relation (31) can be approximated by

$$\Omega^4 - \Omega^2(1 - \langle \beta^2 \rangle) - (\langle \beta^2 \rangle - \langle \beta \rangle^2) = 0. \tag{32}$$

The solutions to the quadratic Eq. (32) for Ω^2 are given by

$$\Omega^2 = \frac{1}{2}(1-\langle\beta^2\rangle)\left[1 \pm \left(1 + \frac{4(\langle\beta^2\rangle - \langle\beta\rangle^2)}{(1-\langle\beta^2\rangle)^2}\right)^{1/2}\right]. \tag{33}$$

It is readily shown from the definitions in Eq. (30) that $\langle\beta^2\rangle \geqslant \langle\beta\rangle^2$. Therefore the upper sign in Eq. (33) corresponds to stable plasma oscillations ($\Omega^2 > 0$) modified by axial streaming effects. On the other hand, for $\langle\beta^2\rangle > \langle\beta\rangle^2$ the lower sign in Eq. (33) corresponds to $\Omega^2 < 0$. Because $\Omega^2 < 0$ for the lower sign in Eq. (33), it follows that $\mathrm{Re}\,\Omega = 0$ and

$$\mathrm{Im}\,\Omega = \pm\frac{1}{\sqrt{2}}(1-\langle\beta^2\rangle)^{1/2}\left[\left(1 + \frac{4(\langle\beta^2\rangle - \langle\beta\rangle^2)}{(1-\langle\beta^2\rangle)^2}\right)^{1/2} - 1\right]^{1/2}. \tag{34}$$

The upper sign in Eq. (34) corresponds to temporal growth (Weibel instability) with $\mathrm{Im}\,\Omega > 0$. Whenever the inequality

$$\frac{4(\langle\beta^2\rangle - \langle\beta\rangle^2)}{(1-\langle\beta^2\rangle)^2} \ll 1 \tag{35}$$

is satisfied, note that the growth rate for the unstable (upper) branch in Eq. (34) is given approximately by

$$\mathrm{Im}\,\Omega = \frac{[\langle\beta^2\rangle - \langle\beta\rangle^2]^{1/2}}{(1-\langle\beta^2\rangle)^{1/2}}. \tag{36}$$

In dimensional units, when the inequality in Eq. (35) is satisfied it follows from Eqs. (30) and (36) that the growth rate of the Weibel instability for short-wavelength perturbations ($c^2k_\perp^2 \gg \sum_{j=b,e,i}\hat{\omega}_{pj}^{i^2}$) in a beam–plasma-filled waveguide can be approximated by

$$\mathrm{Im}\,\omega \simeq \Gamma_{\mathrm{W}} \equiv \frac{[\langle\beta^2\rangle - \langle\beta\rangle^2]^{1/2}}{(1-\langle\beta^2\rangle)^{1/2}}\left(\sum_{j=b,e,i}\hat{\omega}_{pj}^{i^2}\right)^{1/2}. \tag{37}$$

The quantity Γ_{W} defined in Eq. (37) provides a convenient unit in which to measure the growth rate of the Weibel instability in the subsequent numerical analysis of the general dispersion relation (26).

For a beam–plasma-filled waveguide, the exact solutions for ω^2 (or Ω^2) are of course determined from the cubic dispersion relation (29), or equivalently Eq. (31). With regard to the Weibel instability growth rate estimate in Eq. (36) or Eq. (37), it is important to recognize the relative size of the contributions from the various beam–plasma species to the instability drive terms in Eq. (37). For present purposes, we consider a positively charged ion beam ($j = b$) propagating through background plasma electrons and ions ($j = e, i$). The charge states are denoted by $e_b = +Z_be$, $e_e = -e$, and $e_i = +Z_ie$, and the plasma electrons are assumed to carry the neutralizing current ($\beta_e \neq 0$), whereas the plasma ions are taken to be stationary ($\beta_i = 0$). The conditions for charge neutralization, $\sum_{j=b,e,i}\hat{n}_j^i e_j = 0$, and current neutralization, $\sum_{j=b,e,i}\hat{n}_j^i e_j\beta_j = 0$, then give

$$\hat{n}_e^i = Z_b\hat{n}_b^i + Z_i\hat{n}_i^i$$
$$\beta_e = \frac{\beta_b Z_b\hat{n}_b^i}{Z_b\hat{n}_b^i + Z_i\hat{n}_i^i}. \tag{38}$$

Except for the case of a very tenuous beam ($Z_b\hat{n}_b^i \ll Z_i\hat{n}_i^i$), note from Eq. (38) that β_e can be a substantial fraction of β_b.

In the subsequent analysis of the dispersion relations (26) and (29), it is useful to define

$$\Omega_p^{i2} \equiv \sum_{j=b,e,i}\hat{\omega}_{pj}^{i2}, \quad \Omega_p^{o2} \equiv \sum_{j=e,i}\hat{\omega}_{pj}^{o2}, \tag{39}$$

where $\hat{\omega}_{pj}^{i^2} = 4\pi\hat{n}_j^i e_j^2/\gamma_j m_j$, $\gamma_j = (1-\beta_j^2)^{-1/2}$ and $\hat{\omega}_{pj}^{o^2} = 4\pi\hat{n}_j^o e_j^2/m_j$. Note from Eqs. (30) and (39) that $\sum_{j=b,e,i}\hat{\omega}_{pj}^{i^2}/\gamma_j^2 = \Omega_p^{i^2} - \langle\beta^2\rangle\Omega_p^{i^2}$. Careful examination of the expression for Γ_{W} in Eq. (37) for $\beta_i = 0$ shows that

$$\Gamma_{\mathrm{W}}^2 = \frac{1}{(1-\langle\beta^2\rangle)}\left[\frac{(\beta_e^2\hat{\omega}_{pe}^{i^2} + \beta_b^2\hat{\omega}_{pb}^{i^2})\hat{\omega}_{pi}^{i2} + (\beta_b-\beta_e)^2\hat{\omega}_{pe}^{i^2}\hat{\omega}_{pb}^{i^2}}{\sum_{j=b,e,i}\hat{\omega}_{pj}^{i2}}\right]. \tag{40}$$

For $\hat{\omega}_{pb}^{i^2}, \hat{\omega}_{pi}^{i^2} \ll \hat{\omega}_{pe}^{i^2}$, it follows that Eq. (40) is given to good approximation by

$$\Gamma_{\mathrm{W}}^2 \simeq \frac{1}{(1-\beta_e^2)}[\beta_e^2\hat{\omega}_{pi}^{i^2} + (\beta_b-\beta_e)^2\hat{\omega}_{pb}^{i^2}]. \tag{41}$$

Note from Eq. (41) that Γ_{W} involves the (slow) plasma frequencies of both the beam ions and the plasma ions.

In the remainder of Section 3 we consider the case of a cesium ion beam with $Z_b = 1$ and $\beta_b = 0.2$ propagating through a neutralizing background argon plasma with $Z_i = 1$, $\hat{n}_i^i = (1/2)\hat{n}_e^i = \hat{n}_b^i$, and $\beta_e = 0.1$ (see Eq. (38)). Illustrative stability results obtained from Eq. (26) are shown in Figs. 2–4 for the case of a beam–plasma-filled waveguide, where the exact dispersion relation assumes the simple form in Eq. (29) with $k_\perp^2 = p_{0n}^2/r_{\mathrm{w}}^2$, $n = 1, 2, \ldots$, and $J_0(p_{0n}) = 0$. In particular, Figs. 2 and 4 show plots of the normalized growth rate $(\mathrm{Im}\,\omega)/\Gamma_{\mathrm{W}}$ for the unstable branch versus radial mode number n for the choice of parameters corresponding to $\Omega_p^i r_b/c = 1/3$ (Fig. 2) and $\Omega_p^i r_b/c = 3$ (Fig. 4). The corresponding plots of the radial eigenfunction $\delta E_z(r)$ versus r/r_{w} are also shown for mode number $n = 5$. Comparing Figs. 2 and 4, we note that the normalized growth rate for small values of n tends to be smaller for larger values of $\Omega_p^i r_b/c$. In general, for sufficiently large n, the instability growth rate asymptotes at $\mathrm{Im}\,\omega \simeq \Gamma_{\mathrm{W}}$, as expected from the estimate in Eq. (37). Fig. 3 shows a plot of the normalized real frequency $(\mathrm{Re}\,\omega)/\Omega_p^i$ versus radial mode number n obtained from Eq. (26) for the stable fast-wave branch. The system parameters in Fig. 3 is identical to those in Fig. 2, with $\Omega_p^i r_b/c = 1/3$. As expected, in Fig. 3 $(\mathrm{Re}\,\omega)/\Omega_p^i$ asymptotes at $ck_\perp/\Omega_p^i$ for large values of n, where $k_\perp^2 = p_{0n}^2/r_{\mathrm{w}}^2$.

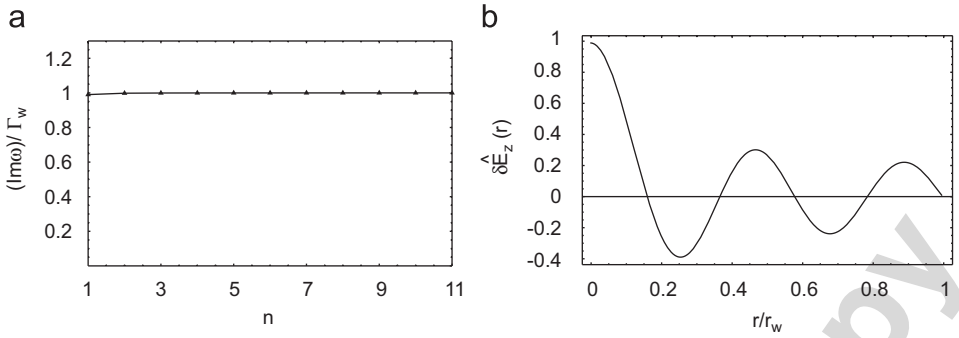

Fig. 2. Plots of (a) Weibel instability growth rate $(\mathrm{Im}\,\omega)/\Gamma_W$ versus mode radial number n, and (b) eigenfunction $\delta\hat{E}_z(r)$ versus r/r_w for $n=5$ obtained from Eq. (26). System parameters are $r_b=r_w$, $\beta_b=0.2$, $\beta_e=0.1$, $\hat{n}_i^i=\hat{n}_e^i/2=\hat{n}_b^i$, and $\Omega_p^i r_b/c=1/3$.

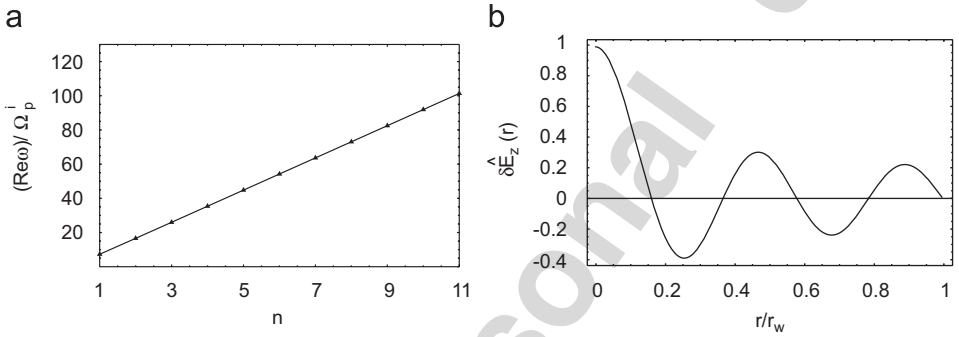

Fig. 3. Plots of (a) stable fast-wave oscillation frequency $(\mathrm{Re}\,\omega)/\Omega_p^i$ versus radial mode number n, and (b) eigenfunction $\delta\hat{E}_z(r)$ versus r/r_w for $n=5$ obtained from Eq. (26). System parameters are $r_b=r_w$, $\beta_b=0.2$, $\beta_e=0.1$, $\hat{n}_i^i=\hat{n}_e^i/2=\hat{n}_b^i$, and $\Omega_p^i r_b/c=1/3$.

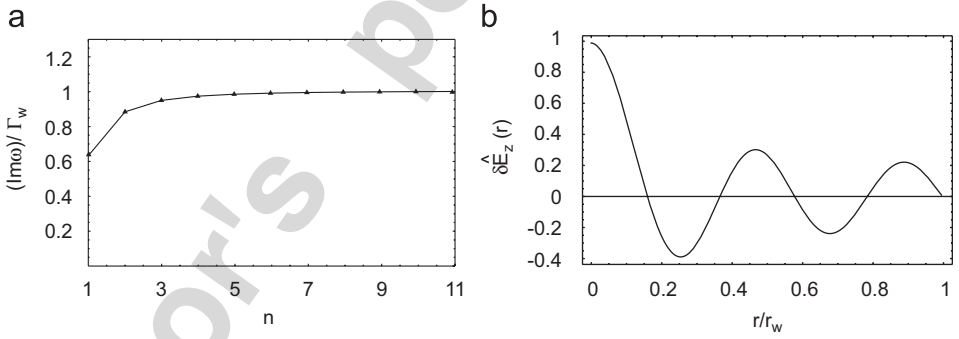

Fig. 4. Plots of (a) Weibel instability growth rate $(\mathrm{Im}\,\omega)/\Gamma_W$ versus radial mode number n, and (b) eigenfunction $\delta\hat{E}_z(r)$ versus r/r_w for $n=5$ obtained from Eq. (26). System parameters are $r_b=r_w$, $\beta_b=0.2$, $\beta_e=0.1$, $\hat{n}_i^i=\hat{n}_e^i/2=\hat{n}_b^i$, and $\Omega_p^i r_b/c=3$.

3.2. Vacuum region outside of beam–plasma channel ($r_b<r_w$; $\hat{n}_j^o=0$, $j=e,i$)

We now consider the case where there is a vacuum region outside the beam–plasma channel, i.e., $r_b<r_w$ and $\hat{n}_j^o=0$, $j=e,i$. In this case $T_o^2(\omega)=-\omega^2/c^2$ and $\Omega_p^{o2}=0$ follow from Eqs. (20) and (39), and the full transcendental dispersion relation (26) must be solved numerically. As before, both stable (fast-wave and plasma oscillation) and unstable (Weibel-like) solutions are found. For brevity, we focus here on the unstable solutions to Eq. (26). Typical numerical solutions to Eq. (26) are illustrated in Figs. 5 and 6 for the choice of system parameters $r_w=3r_b$, $\beta_b=0.2$, $\beta_e=0.1$, $\hat{n}_i^i=\hat{n}_e^i/2=\hat{n}_b^i$, $\Omega_p^o=0$ and $\Omega_p^i r_b/c=1/3$ (Fig. 5) and $\Omega_p^i r_b/c=3$ (Fig. 6). Shown in Figs. 5 and 6 are plots of the normalized growth rate $(\mathrm{Im}\,\omega)/\Gamma_W$ versus radial mode number n, and plots of the eigenfunction $\delta E_z(r)$ versus r/r_w for mode number $n=5$. Note from Figs. 5 and 6 that the signature of the instability growth rate for the case of a vacuum region outside the beam–plasma channel is qualitatively similar to that in Figs. 2 and 4 for the case of a beam–plasma-filled waveguide. However, the normalized growth rate in Fig. 6 is somewhat larger for lower values of radial mode number n than that in Fig. 4.

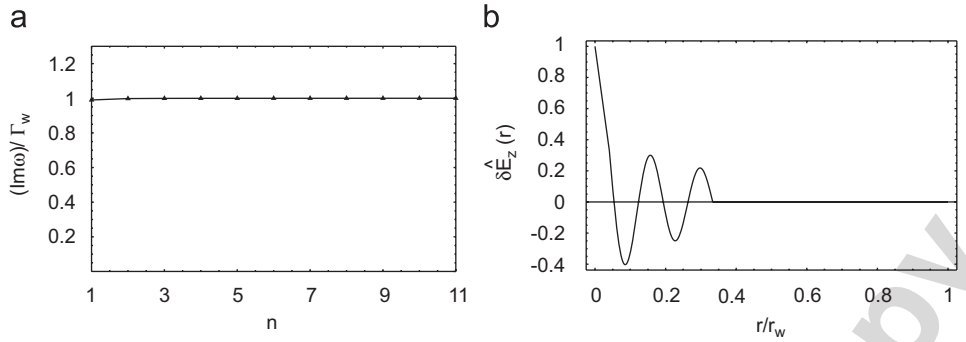

Fig. 5. Plots of (a) Weibel instability growth rate $(\mathrm{Im}\,\omega)/\Gamma_W$ versus radial mode number n, and (b) eigenfunction $\delta\hat{E}_z(r)$ versus r/r_w for $n=5$ obtained from Eq. (26). System parameters are $r_b=r_w/3$, $\beta_b=0.2$, $\beta_e=0.1$, $\hat{n}_i^i=\hat{n}_e^i/2=\hat{n}_b^i$, $\Omega_p^i r_b/c=1/3$ and $\Omega_p^o=0$.

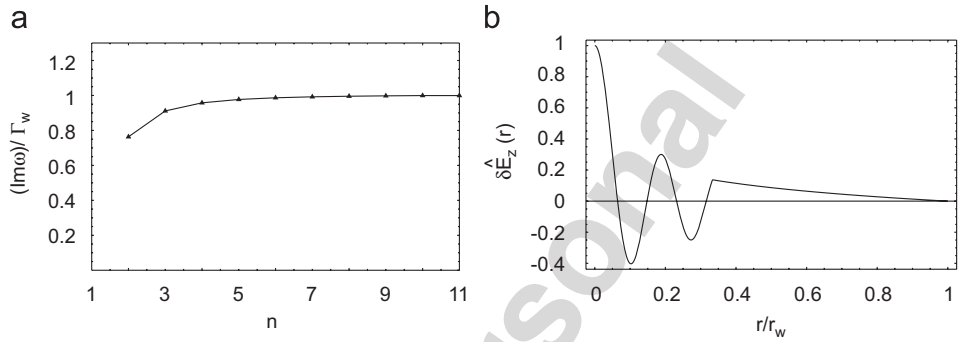

Fig. 6. Plots of (a) Weibel instability growth rate $(\mathrm{Im}\,\omega)/\Gamma_W$ versus radial mode number n, and (b) eigenfunction $\delta\hat{E}_z(r)$ versus r/r_w for $n=5$ obtained from Eq. (26). System parameters are $r_b=r_w/3$, $\beta_b=0.2$, $\beta_e=0.1$, $\hat{n}_i^i=\hat{n}_e^i/2=\hat{n}_b^i$, $\Omega_p^i r_b/c=3$ and $\Omega_p^o=0$.

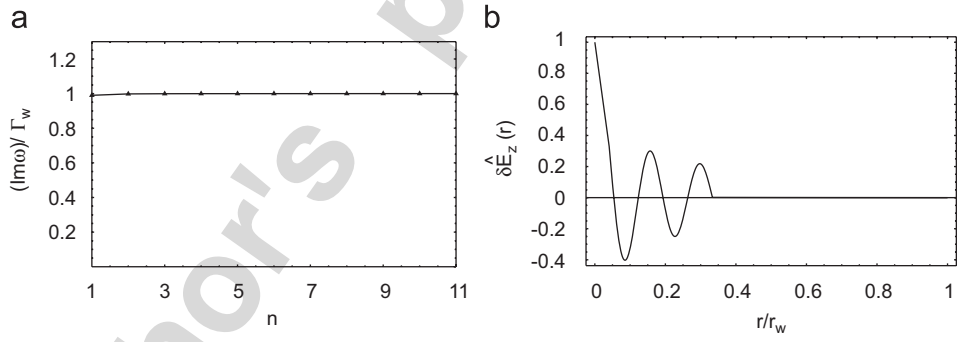

Fig. 7. Plots of (a) Weibel instability growth rate $(\mathrm{Im}\,\omega)/\Gamma_W$ versus radial mode number n, and (b) eigenfunction $\delta\hat{E}_z(r)$ versus r/r_w for $n=5$ obtained from Eq. (26). System parameters are $r_b=r_w/3$, $\beta_b=0.2$, $\beta_e=0.1$, $\hat{n}_i^i=\hat{n}_e^i/2=\hat{n}_b^i=\hat{n}_e^o=\hat{n}_i^o$, $\Omega_p^i r_b/c=1/3$.

3.3. *Plasma outside of beam–plasma channel* ($r_b<r_w$; $\hat{n}_j^o\neq 0$, $j=e,i$)

We now consider the dispersion relation (26) for the case where there is plasma outside the beam–plasma channel, i.e., $r_b<r_w$ and $\hat{n}_j^o\neq 0$, $j=e,i$. In this case $T_o^2(\omega)=-(\omega^2/c^2-\Omega_p^{o2}/c^2)$, where $\Omega_p^{o2}=\sum_{j=e,i}\hat{\omega}_{pj}^{o2}$. Typical numerical solutions to Eq. (26) for the unstable branch are illustrated in Figs. 7 and 8 for the choice of system parameters $r_w=3r_b$, $\beta_b=0.2$, $\beta_e=0.1$, $\hat{n}_i^i=\hat{n}_e^i/2=\hat{n}_b^i=\hat{n}_e^o=\hat{n}_i^o$, and $\Omega_p^i r_b/c=1/3$ (Fig. 7) and $\Omega_p^i r_b/c=3$ (Fig. 8). Shown in Figs. 7 and 8 are plots of the normalized growth rate $(\mathrm{Im}\,\omega)/\Gamma_W$ versus radial mode number n, and plots of the eigenfunction $\delta E_z(r)$ versus r/r_w for mode number $n=5$. Comparing Fig. 5 with Fig. 7, and Fig. 6 with Fig. 8, it is evident that the inclusion of plasma outside the beam–plasma channel does not significantly change the instability growth rate relative to the case where there is vacuum outside the beam–plasma channel.

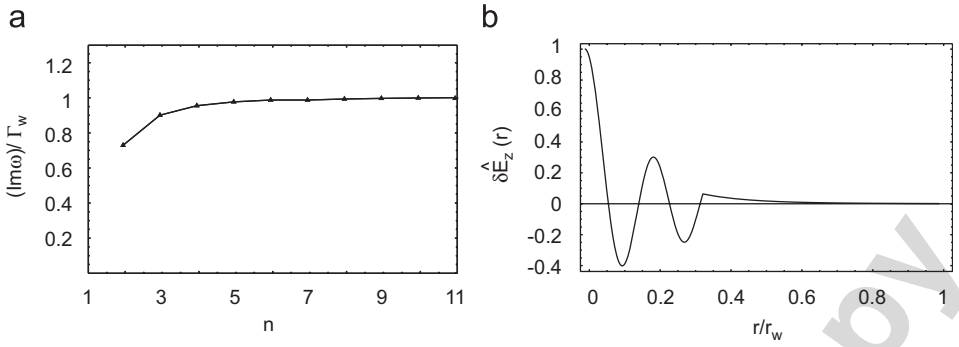

Fig. 8. Plots of (a) Weibel instability growth rate $(\mathrm{Im}\,\omega)/\Gamma_W$ versus radial mode number n, and (b) eigenfunction $\delta\hat{E}_z(r)$ versus r/r_w for $n=5$ obtained from Eq. (26). System parameters are $r_b = r_w/3$, $\beta_b = 0.2$, $\beta_e = 0.1$, $\hat{n}_i^i = \hat{n}_e/2 = \hat{n}_b^i = \hat{n}_e^o = \hat{n}_i^o$, $\Omega_p^i r_b/c = 3$.

4. Conclusions

In this paper we made use of a macroscopic cold-fluid model to investigate detailed properties of the multi-species electromagnetic Weibel instability (Sections 2 and 3) for an intense ion beam propagating through a background plasma that provides complete charge and current neutralization. Detailed growth-rate properties have been calculated for a wide range of system parameters. To summarize, it is clear from the analysis in Section 3 that the multispecies Weibel instability with characteristic growth rate Γ_W can be particularly virulent for a sufficiently intense (high density) ion charge bunch propagating through background plasma that provides complete charge and current neutralization. On the other hand, the multi-species Weibel instability is unlikely to have a deleterious effect on the beam quality provided

$$\Gamma_W \tau_p < 1 \tag{42}$$

where $\tau_p = L_p/V_b$ is the interaction time of the beam ions with the background plasma, and L_p is the length of the plasma column. Equivalently, $\Gamma_W \tau_p < 1$ gives

$$L_p < \alpha \frac{c}{\hat{\omega}_{pb}^i} = 2.3 \times 10^7 \alpha \frac{A_b^{1/2}}{[\hat{n}_b^i(\mathrm{cm}^{-3})]^{1/2}}\,\mathrm{cm} \tag{43}$$

where use is made of Eq. (41), and the constant α is defined in the nonrelativistic case by

$$\alpha = \left[\left(1 - \frac{Z_b \hat{n}_b^i}{\hat{n}_e^i}\right)^2 + \frac{Z_i m_b}{Z_b m_i}\frac{Z_b \hat{n}_b^i}{\hat{n}_e^i}\left(1 - \frac{Z_b \hat{n}_b^i}{\hat{n}_e^i}\right)\right]^{-1/2}. \tag{44}$$

For singly-ionized Aluminum beam ions ($Z_b = 1$ and $A_b = 13$) in background Argon plasma ($A_i = 18$) and $\hat{n}_b^i/\hat{n}_e^i = 1/2$, we obtain from Eqs. (43) and (44) that

$$L_p < 1.27\,\mathrm{m}, \quad 12.7\,\mathrm{m}, \quad 127\,\mathrm{m} \tag{45}$$

for

$$\hat{n}_b^i = 10^{12}\,\mathrm{cm}^{-3}, \quad 10^{10}\,\mathrm{cm}^{-3}, \quad 10^{8}\,\mathrm{cm}^{-3}. \tag{46}$$

Therefore, from Eqs. (43)–(46), the exponentiation length for the multispecies Weibel instability is moderately long, even for beam densities in the range $10^{10}\,\mathrm{cm}^{-3} - 10^{12}\,\mathrm{cm}^{-3}$.

Finally, it should be pointed out that the relative importance of the electrostatic two-stream and electromagnetic Weibel instabilities for similar system parameters has been briefly discussed in Ref. [3].

Acknowledgments

This research was supported by the U.S. Department of Energy.

References

[1] R.C. Davidson, H. Qin, Physics of Intense Charged Particle Beams in High Energy Accelerators, World Scientific, Singapore, 2001 and references therein.
[2] M. Reiser, Theory and Design of Charged Particle Beams, Wiley, New York, 1994.
[3] R.C. Davidson, I. Kaganovich, H. Qin, E.A. Startsev, D.R. Welch, D.V. Rose, H.S. Uhm, Phys. Rev. ST Accel. Beams 7 (2004) 114801.
[4] H. Qin, Phys. Plasmas 10 (2003) 2708.
[5] R.C. Davidson, A. Friedman, C.M. Celata, D.R. Welch, et al., Laser Part. Beams 20 (2002) 377.
[6] R.C. Davidson, B.G. Logan, J.J. Barnard, et al., Journal de Physique France 133 (2006) 731.
[7] E.G. Harris, Phys. Rev. Lett. 2 (1959) 34.
[8] E.A. Startsev, R.C. Davidson, H. Qin, Phys. Rev. ST Accel. Beams 8 (2005) 124201.
[9] E.A. Startsev, R.C. Davidson, H. Qin, Phys. Rev. ST Accel. Beams 6 (2003) 084401.
[10] E.A. Startsev, R.C. Davidson, H. Qin, Laser Part. Beams 20 (2002) 585.
[11] E.A. Startsev, R.C. Davidson, H. Qin, Phys. Plasmas 9 (2002) 3138.
[12] I. Haber, A. Friedman, D.P. Grote, S.M. Lund, R.A. Kishek, Phys. Plasmas 6 (1999) 2254.
[13] A. Friedman, D.P. Grote, I. Haber, Phys. Fluids B 4 (1992) 2203.
[14] E.S. Weibel, Phys. Rev. Lett. 2 (1959) 83.
[15] E.A. Startsev, R.C. Davidson, Phys. Plasmas 10 (2003) 4829.
[16] M. Honda, J. Meyer-ter-Vehn, A. Pukhov, Phys. Rev. Lett. 85 (2000) 2128.
[17] C.A. Kapetanakos, Appl. Phys. Lett. 25 (1974) 484.
[18] R. Lee, M. Lampe, Phys. Rev. Lett. 31 (1973) 1390.
[19] R.C. Davidson, D.A. Hammer, I. Haber, C.E. Wagner, Phys. Fluids 15 (1972) 317.
[20] V.K. Neil, A.M. Sessler, Rev. Sci. Instr. 36 (1965) 429.
[21] R.C. Davidson, H. Qin, G. Shvets, Phys. Rev. ST Accel. Beams 6 (2003) 104402.
[22] E.P. Lee, Part. Acceler. 37 (1992) 307.

[23] R.J. Macek, et al., Proceedings of the 2001 Particle Accelerator Conference, vol. 1, 2001, p. 688.
[24] H. Qin, E.A. Startsev, R.C. Davidson, Phys. Rev. ST Accel. Beams 6 (2003) 014401.
[25] T.-S. Wang, P.J. Channell, R.J. Macek, R.C. Davidson, Phys. Rev. ST Accel. Beams 6 (2003) 014204.
[26] H. Qin, R.C. Davidson, E.A. Startsev, W.W. Lee, Laser Part. Beams 21 (2003) 21.
[27] R.C. Davidson, H.S. Uhm, Phys. Lett. A 285 (2001) 88.
[28] H. Qin, R.C. Davidson, W.W. Lee, Phys. Rev. ST Accel. Beams 3 (2000) 084401;
H. Qin, R.C. Davidson, W.W. Lee, Phys. Rev. ST Accel. Beams 3 (2000) 109901.
[29] R.C. Davidson, H. Qin, Phys. Lett. A 270 (2000) 177.
[30] R.C. Davidson, H. Qin, P.H. Stoltz, T.-S. Wang, Phys. Rev. ST Accel. Beams 2 (1999) 054401.
[31] M.N. Rosenbluth, Phys. Fluids 3 (1960) 932.
[32] H.S. Uhm, R.C. Davidson, IEEE Trans. Plasma Sci. 33 (2005) 1395.
[33] H.S. Uhm, R.C. Davidson, Phys. Rev. ST Accel. Beams 6 (2003) 034204.
[34] R.F. Fernsler, S.P. Slinker, M. Lampe, R.F. Hubbard, Phys. Plasmas 2 (1995) 4338 and references therein.
[35] H.S. Uhm, M. Lampe, Phys. Fluids 24 (1981) 1553.
[36] E.P. Lee, Phys. Fluids 21 (1978) 1327.
[37] H.S. Uhm, R.C. Davidson, I.D. Kaganovich, Phys. Plasmas 8 (2001) 4637.
[38] G. Joyce, M. Lampe, Phys. Fluids 26 (1983) 3377.
[39] H.S. Uhm, R.C. Davidson, Phys. Fluids 23 (1980) 1586.
[40] E.A. Startsev, R.C. Davidson, Phys. Plasmas 13 (2006) 062108.
[41] T.C. Genoni, D.V. Rose, D.R. Welch, E.R. Lee, Phys. Plasmas 11 (2004) L73.
[42] R.C. Davidson, I. Kaganovich, E.A. Startsev, Princeton Plasma Physics Laboratory Report No. 3940, 2004.
[43] E.P. Lee, S. Yu, H.L. Buchanan, F.W. Chambers, M.N. Rosenbluth, Phys. Fluids 23 (1980) 2095.
[44] P.F. Ottinger, D. Mosher, S.A. Goldstein, Phys. Fluids 24 (1981) 164.
[45] D.V. Rose, T.C. Genoni, D.R. Welch, E.P. Lee, Nucl. Instr. and Meth. A 544 (2005) 389.
[46] C. Thoma, D.R. Welch, S.S. Yu, E. Henestroza, P.K. Roy, S. Eylon, E.P. Gilson, Phys. Plasmas 12 (2005) 043102.
[47] P.K. Roy, S.S. Yu, E. Henestroza, et al., Phys. Rev. Lett. 95 (2005) 234801.
[48] A.B. Sefkow, R.C. Davidson, P.C. Efthimion, et al., Phys. Rev. ST Accel. Beams 9 (2006) 052801.
[49] R.C. Davidson, H. Qin, Phys. Rev. ST Accel. Beams 8 (2005) 064201.
[50] I.D. Kaganovich, G. Shvets, E. Startsev, R.C. Davidson, Phys. Plasmas 8 (2001) 4180.
[51] I. Kaganovich, E.A. Startsev, R.C. Davidson, Laser Part. Beams 20 (2002) 497.
[52] D.R. Welch, D.V. Rose, B.V. Oliver, T.C. Genoni, C.L. Olson, S.S. Yu, Phys. Plasmas 9 (2002) 2344.
[53] A. Pukhov, J. Meyer-ter-Vehn, Phys. Rev. Lett. 79 (1997) 2686.
[54] R. Jung, J. Osterholtz, et al., Phys. Rev. Lett. 94 (2005) 195001.
[55] T. Taguchi, T.M. Antonsen Jr., C.S. Liu, K. Mima, Phys. Rev. Lett. 86 (2001) 5055.
[56] M. Tabak, J. Hammer, M.E. Glinsky, et al., Phys. Plasmas 1 (1994) 1626.
[57] R.C. Davidson, Physics of Nonneutral Plasmas, World Scientific, 2001.
[58] See, for example, pp. 272–276 of Ref. [57].